Heliyon 10 (2024) e24911

Contents lists available at ScienceDirect

Heliyon

journal homepage: www.cell.com/heliyon

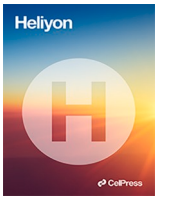

Research article

Response of hydrological ecosystem services to land-use change and risk assessment in Jiangxi Province, China

Chun Fu, Yezhong Liu *, Fan Li, Huimin Huang, Shuchen Zheng

School of Infrastructure Engineering, Nanchang University, Nanchang, 330031, China

ARTICLE INFO

Keywords:
Land use change
PLUS model
Hydrological ecosystem services
Land use prediction
Jiangxi

ABSTRACT

Water bodies provide humans with important hydrological ecosystem services (HESs), directly or indirectly. Water yield, water conservation, and soil conservation are essential to HESs. Since China's reform and opening up, and with its rapid socio-economic development, land use in Jiangxi Province has undergone drastic change, resulting in threats to the ecological environment. This paper evaluates three HESs, water yield, water conservation, and soil conservation, in Jiangxi Province based on land use and rainfall data, quantifies the impacts of different land classes on each ecosystem, predicts future land use using the patch-generating land use simulation (PLUS) model, and finally, discusses the ecological risks in the study area. The following results were obtained: (1) The HESs in the basin increased and then decreased from 2000 to 2020, and the spatial distribution of water yield and water conservation was greatly influenced by rainfall. Soil conservation was mostly consistent with the elevation distribution. (2) Over time, the overall aggregation of HESs in the study area increased. There were small differences in the effects of various land uses on water yield and water conservation, and large differences in the effects on soil conservation. (3) The distribution of ecological risks was not affected by different land use strategies, with the lower ecological risk level 1 dominating. Most risk areas were present in Ganzhou, Ji'an, Shangrao, and Jiujiang. The ecological risk from urban sprawl (US) accounted for the most significant proportion, and that from the ecological protection (EP) strategy accounted for the lowest proportion. This study provides reference for sustainable land use development and ecological risk prevention in the study area.

1. Introduction

Hydrological ecosystem services (HESs) refer to the products and functions provided by water bodies that benefit human beings and contribute to their survival [1,2]. These services are essential for maintaining and improving ecosystems and achieving sustainable regional development [3]. Due to climate change and human activities, these ecosystem services are declining or becoming degraded, thereby posing a threat to human safety and health [4]. More than two-thirds of ecosystem services, globally, are declining, and this is expected to continue over the next 50 years [5]. Since the reform and opening up, China has been seeing a rapid economic and population growth, leading to accelerated urbanization. Land use planning as a result of urbanization is leading to changes in land use patterns. Land use, a form of human activity that influences the environment, is growing in intensity. In some areas, uncontrolled development with extensive land use changes have brought both growth and economic benefits but entail the destruction of the

* Corresponding author.
E-mail address: lu3134656529@foxmail.com (Y. Liu).

https://doi.org/10.1016/j.heliyon.2024.e24911
Received 22 September 2023; Received in revised form 21 December 2023; Accepted 17 January 2024
Available online 18 January 2024

ecological environment, leading to issues such as greenhouse gas emissions, floods, soil erosion, and land desertification, among others. Given the limited water resources, rapid economic and social development, and continuous land use changes, China's aquatic ecosystems are facing various challenges [6] such as water shortage, pollution and deterioration of water, uneven spatial and temporal distribution of water resources, supply and demand imbalances, and frequent floods and disasters. Land use is the basis of human development, and efficient land use planning can help solve sustainable problems [7]. Many studies have shown that land use change is one of the most important factors affecting ecosystem services [8]. Sannigrahi et al. [9] calculated the effect of land use change on the global ecosystem service value from 1995 to 2015. They found that deforestation and depletion of wetlands and water surfaces resulted in a net ecosystem service value loss of $1.21 trillion. Kindu et al. [10] analyzed the response of ecosystem services to land use change in the Ethiopian highlands. They found a decline in the value of ecosystem services in the study area as a result of land use changes by human activity. Ning et al. [11] and Zhang [12] suggested that by implementing ecological projects such as returning cultivated land to forests, vegetation cover could be increased, and as a result, ecosystem services such as water conservation could be improved.

At this stage, although land use models are continuously being optimized and improved, some models remain deficient at simulating the spatiotemporal dynamic evolution of different land use types at the patch scale, and it is difficult to explain the relationships among land use types. For example, with the CA-Markov model, simulation of the spatiotemporal dynamics of natural land type patch changes is difficult. It needs to be revised, therefore, in terms of the land use transformation rules. The CLUE-S and FLUS models are not sufficiently accurate [13]. The patch-generating land use simulation (PLUS) model adopts the land expansion analysis strategy (LEAS) rule framework and the multi-type stochastic seeded CA model [14], with which the causal factors of various types of land use changes can be better explored compared to other models [15], particularly in terms of patch-level changes of natural landscapes, such as grasslands and forest land [16]. The model also includes the multi-objective optimization algorithm. Compared with other CA models, therefore, the PLUS model has higher accuracy [17], and the simulation results better support the development of targeted future planning policies.

HES accounting is mainly divided into the assessment of quantitative value and the assessment of ecological modeling approaches. Because the estimate of quantitative value is mainly embodied in assessing the value coefficient, the method tends to be subjective [18]. The environmental modeling approach, however, relies on the calculation of physical ecosystem services, and is therefore more objective in terms of ecosystem service accounting. The main models used for ecosystem service accounting are the InVEST, ARIES, SoIVES, and MIMES. Montse et al. [19] used the InVEST model to assess the water yield of the Franconia River Basin in response to the increasingly severe water scarcity. The model provided good results of the HESs in the region affected by climate change. Wang et al. [20] used the InVEST and other models to analyze the spatial differentiation characteristics of three typical HESs, namely, rainfall and flood regulation, soil and water conservation, and water quality purification, in the Taihu Lake Basin and explored the relationships between HESs and the characteristics of different landscape patterns at the sub-basin scale. Bagstad et al. [21] used the ARIES model to analyze simulation maps of carbon sequestration in PSI countries, landscape maps, sediment regulation, and water yield strategies and to inform the development of a new forest plan for the country. Huo et al. [22] assessed the cultural value of ecosystems in southern Wuyi County, Zhejiang Province, based on the SolVES model and the expert survey method. Boumans et al. [23] explained the operation mechanism of MIMES and discussed the advantages and disadvantages of the model in an article published in 2015. Among many models, the InVEST model is the most widely used due to its ease of operation and visualization of results, as well as accuracy of data [24–26].

HESs are usually strongly influenced by changes in climate and human activities. Improving regional HESs despite climate change is, however, difficult due to the global nature and uncertainty of climate change [27]. Land use is one of the most significant manifestations of human activities. The complex response of HESs to land use changes mainly stems from the spatial and temporal heterogeneity [28]. Long-term land use, ecosystem service analyses, and land use management and prediction can, therefore, be more effective in maintaining HESs. Currently, research on ecosystem services focuses on current and historical trends, but there is a relative lack of future projections. In addition, research on HES changes and risks associated with specific land types is relatively limited. It is, therefore, necessary to explore the relationship between land use and ecosystem services in greater depth, to quantify the links between various land use types and HESs, and to model the distribution of ecosystem services and risks under different future strategies.

The Poyang Lake watershed, a critical watershed in the middle and lower reaches of the Yangtze River, plays a crucial role in flood control, biodiversity conservation, and soil preservation. Jiangxi Province occupies 94 % of the Poyang Lake Basin area, so the land use change in this area has an essential impact on the ecological status and sustainable development of the whole basin. In recent years, the rapid economic and social growth of Jiangxi Province has led to remarkable changes in land use. Studying the impacts of land use on HESs in the region is of practical significance as it helps plan the region's future development and provides effective strategies for ecological environmental management. In the present study, the InVEST and PLUS models were used to assess three HESs, that is, water yield, water conservation, and soil conservation, in Jiangxi Province and to quantify the specific effects of various types of land use on ecosystem services. In addition, the effects of different land use types on ecosystem services were analyzed under different land strategies. Finally, the ecological risks in the study area were classified based on an ecosystem service assessment. The results of this study provide an important reference for future development and land use planning in the Poyang Lake area, and will help guide policy formulation and regional planning as well as promote a coordinated development of ecological protection and sustainable development.

2. Materials and methods

2.1. Study area

Jiangxi Province (113°34′E–118°28′E, 24°29′N-30°04′N) is located in the center of southeastern China, on the south bank of the middle and lower reaches of the Yangtze River, with a topography of high in the south and low in the north, and belongs to the middle subtropical region (Fig. 1), with a distinct monsoon climate, showing the climate characteristics of four different seasons [29]. The geographical scope of Jiangxi Province is highly compatible with the Poyang Lake Basin. The total area of the province is 166,900 km^2, of which 156,743 km^2 belong to the Poyang Lake Basin, accounting for 96.9 % of the total area of the basin. The five major rivers in the province converge into Poyang Lake in a radial shape; thus, the water resources in the province mainly depend on rainfall, which leads to apparent changes in water resources in different seasons, with abundant water resources in the rainy season, which is prone to flooding, and the challenge of scarce water resources in the dry season. In recent years, as urbanization continues, land use in Jiangxi Province has changed dramatically, posing a potential threat to HES.

2.2. Data sources

We selected five data periods, 2000, 2005, 2010, 2015, and 2020, as the time series for the study. The primary data used were land use data, watershed boundary data, protected area boundary data, daily rainfall data, potential evapotranspiration data, soil data, data on the available water content of vegetation, biophysical coefficients table and runoff coefficients, DEM, Rainfall erosivity factor, soil erosivity factor, etc. All raster data were regionally cropped using ArcGIS 10.2. The land use data are divided into six categories: cultivated land, forest land, grassland, water area, building land, and unused land, according to the secondary classification of the Resource and Environment Science and Data Center. The coordinate system of all data is uniformly Krasovsky_1940_Albers, and the resolution is uniformly 1 km × 1 km. Specific data sources are listed in Table 1.

2.3. Methods

2.3.1. Calculation of HESs

2.3.1.1. Water yield. In this study, the water yield module of the InVEST model was used to estimate the water yield of the study area based on the water balance principle and the Budyko curve, and the main calculation principles is shown in equation (1):

$$Y_x = \left(1 - \frac{AET_x}{P_x}\right) \times P_x \tag{1}$$

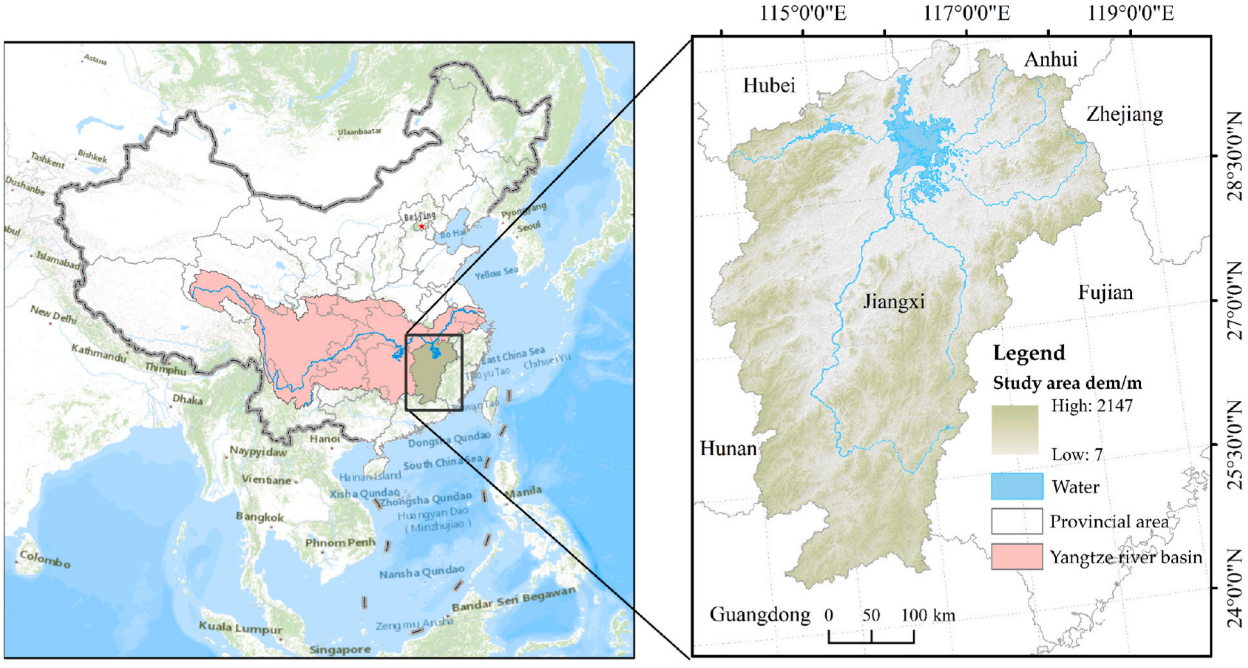

Fig. 1. Geographical location and profile of the study area.

Table 1
Data source and interpretation.

Module	Data	Data source or reference	Format
Land use simulation	Land use data for 2000–2020	Resource Environmental Science and Data Centre (https://www.resdc.cn/)	.tif
	DEM data, based on DEM data, slope, and aspect data obtained through ArcGIS 10.2 surface analysis	Geospatial Data Cloud (https://www.gscloud.cn/)	.tif
	Railways, national roads and motorways, waterways	Geo-monitoring cloud platform (http://www.dsac.cn/)	.shp
	GDP data, population data for 2010 and 2015: obtained by inverse distance weighting method difference	Jiangxi Provincial Statistical Yearbook, Seventh Population Census	.tif
	Watershed limitation area data and protected area boundaries	National Earth System Science Data Centre (http://www.geodata.cn/)	.shp
Water yield and water conservation	Daily rainfall data: obtained by interpolation using the inverse distance weighting method	China Meteorological Data Network (https://data.cma.cn/)	.tif
	Potential evapotranspiration data	National Earth System Science Data Centre (http://www.geodata.cn)	.tif
	Soil data	Harmonized World Soil Database	.tif
	Vegetation available water content (PAWC)	Reference [30]	.tif
	Table of biophysical coefficients	InVEST User Guide [31–34]	.csv
Soil conservation	Rainfall erosivity factor R	Reference [35]	.tif
	Soil erodibility factor K	EPIC model [36]	.tif
	Table of biophysical coefficients: vegetation cover factor C, soil conservation measures factor P	InVEST User Guide [31]; References [37,38]	.csv

where Y_x is the annual water yield (mm) of grid x; AET_x is the actual yearly evapotranspiration (mm) of grid x; P_x is the annual precipitation (mm) of grid x; and PET_x is the potential evapotranspiration (mm).

2.3.1.2. Water conservation. Based on the results of the water yield analysis calculation into, we use the principle of water balance to calculate the water conservation volume. The calculation of runoff volume refers to the method in the "*Guidelines for the Delineation of Ecological Protection Red Line*" [39], the specific calculation formulas are shown in equations (2) and (3):

$$R_x = P_x \times \alpha \tag{2}$$

$$W_x = Y_x - R_x \tag{3}$$

where W_x is the amount of water conservation in x years; R_x is the amount of runoff (mm) in x years; P_x is the rainfall (mm) in x years; and α is the runoff coefficient.

2.3.1.3. Soil conservation. Soil conservation (SC) is an essential regulating service that refers to ecosystems that work through their structures and processes to reduce soil erosion [40]. We used the Revised Universal Soil Loss Equation (RUSLE) to calculate the Soil conservation, which is more scientific and accurate than the Universal Soil Loss Equation (USLE) equation calculation, as RUSLE considers the plot's ability to intercept upslope soil erosive material [41]. The specific calculation formulas are shown in equation (4) (5) and (6):

$$Q_{sr} = Q_{se\_p} - Q_{se\_\alpha} \tag{4}$$

$$Q_{se\_p} = R \times K \times L \times S \tag{5}$$

$$Q_{se\_\alpha} = R \times K \times L \times S \times P \times C \tag{6}$$

where Q_{sr} is the soil conservation ($t \bullet hm^{-2} \bullet a^{-1}$); Q_{se_p} is the potential soil erosion ($t \bullet hm^{-2} \bullet a^{-1}$); Q_{se_α} is the actual soil erosion ($t \bullet hm^{-2} \bullet a^{-1}$); R is the rainfall erosion factor ($MJ \bullet mm \bullet hm^{-2} \bullet h^{-1} \bullet a^{-1}$); K is the soil erodibility factor ($t \bullet h \bullet MJ^{-1} \bullet mm^{-1}$); L is a dimensionless factor for the length of slopes; S is a dimensionless factor for the slope gradient; C is a dimensionless factor for the vegetation cover; P is a dimensionless factor for the soil and water conservation measures.

2.3.2. Land use modeling

2.3.2.1. Markov volume forecasts. Based on the historical transfer probability matrix of Jiangxi Province from 2010 to 2020, set up the transfer matrices for the three strategies of natural development, urban sprawl, and ecological protection, and predict the quantities of each type of land use under the three strategies in 2030, the formula is shown in equation (7):

$$S_{t+1} = S_t \times p_{ij} \tag{7}$$

where S_{t+1} and St are the land use status at moments $t+1$ and t, respectively, and p_{ij} is the transfer matrix for converting land class i to land class j.

2.3.2.2. PLUS model. The PLUS model integrates two modules: Land expansion analysis strategy (LEAS) and a meta cellular automata (CA) model based on a multi-type stochastic seeding mechanism. LEAS is a superposition of land use data for two periods, 2010 and 2015, to extract cells with change states that represent the change area of each land use type. At the same time, the model adopts a double-decision random forest algorithm to mine each class's expansion and driving factors to obtain the class's development probability and the contribution of the driving factors to the growth of each type. The calculation principle is shown in equation (8):

$$P_{i,k}^{d}(x) = \frac{\sum_{n=1}^{M} I(h_n(x) = d)}{M} \tag{8}$$

where d has a value of 1 or 0; a value of 1 indicates that there is a change from other land use types to land use type k, while 0 means different shifts, x is a vector of multiple drivers, and $I(h_n(x) = d)$ is an indicator function for the set of decision trees; $h_n(x)$ is the predicted type of the nth decision tree for the vector x, and M is the total number of decision trees.

Based on the Markov transfer matrix to obtain the desired future land use quantity and the results of the LEAS module run, then use the CA model based on multi-class stochastic patch seeding, combined with the transfer matrix and domain weights, to influence the local land use competition through adaptive coefficients, and, finally, to drive the land use quantity to meet the future demand. The specific formula is shown in equation (9):

$$OP_{i,k}^{d=1,t} = P_{i,k}^{d=1} \times \Omega_{i,k}^{t} \times D_{k}^{t} \tag{9}$$

where $OP_{i,k}^{d=1,t}$ is the overall probability of land use; $P_{i,k}^{d}$ is the probability of suitability of the land use type at grid i towards k; $\Omega_{i,k}^{t}$ denotes the domain weight of ground class k at grid i at moment t; D_{k}^{t} is the adaptive driving factor.

2.3.2.3. Land strategies setting. Natural development strategy (ND): Without setting any constraints, the land use in 2030 is simulated by following the development rate and land use transfer matrix from 2010 to 2015.

Urban sprawl strategy (US): Based on the natural development Strategy, the US in this paper is mainly used to demonstrate the impacts on HES in the encroachment of agricultural land and eco-friendly land under rapid urban development. Referring to other related articles [42,43], this paper increases the probability of converting cultivated land, forest land, and grassland to building land by 50 % based on the original. It reduces the likelihood of converting building land to other land types by 30 %. The land use area in the US is calculated based on the newly obtained land use transfer probability matrix. In addition, when setting the transfer condition matrix, all building land is set to 0, i.e., no expansion to other land categories.

Ecological protection strategy (EP): Based on the natural development strategy, referring to the relevant research as well as planning [44,45], and other research papers in the study area and Poyang Lake area, the land use transfer probability matrix is set up, and the land use area under this strategy is calculated. In the setup, the conversion of cultivated land, forest land, and grassland to building land is strictly limited; the probability of transferring these three land use categories to building land is reduced by 50 %, and the reduction of cultivated land is increased to forest land. In addition, in the EP land use simulation, based on changing the transfer probability matrix, the nature reserve is added to the restricted area and the water area, which is set to 0 to indicate the restriction of the conversion of land categories.

2.3.3. Hydrological ecological value at risk (HEVR) assessment

The coordinated development status of HES is a comprehensive characterization of regional water ecosystem quality. To assess the water ecological risk situation in different regions, we constructed a water ecological risk assessment HEVR model by calculating a comprehensive index of HESs [42], which can make up for the deficiency of the average index, and comprehensively reflect the variability of each water ecosystem service [46].

Firstly, we standardized the quality of different HESs function objects. Then, we obtained the water ecosystem service index HES_i on grid i by adopting the method of coefficient of divergence. Finally, we obtained the water ecosystem service composite index HES_{com} in the study area by adopting the method of coefficient of divergence. The calculation formulas are shown in equations (10) and (11):

$$HES_i = \frac{\sigma_{ij}}{\bar{x}_{ij}} = \frac{1}{\bar{x}_{ij}} \sqrt{\frac{1}{N} \sum_{j=1}^{N} \left(x_{ij} - \bar{x}_{ij}\right)^2} \tag{10}$$

$$HES_{com} = HES_{(HES_1, HES_2, \ldots HES_n)} \tag{11}$$

Where HES_i is the HES index of the ith raster cell; x_{ij} is the normalized value of the jth type of HES on the ith raster, and $\bar{x}_{ij}$ is its average value; N is the type of HESs computed; and HES_{com} is the composite index of HESs, and the larger the value is, the more significant the difference between the HESs, and the poorer the balance.

We treat conversions beneficial to HESs as forward and unfavorable as reverse conversions. The reverse conversion rate of HES is

represented by calculating the ratio of the area of each HESs reverse conversion to the total study area; the difference between different moments of HES is characterized as the amount of risk loss. The specific formulas are shown in equation (12) (13) and (14):

$$P = \frac{\Delta S}{S} \tag{12}$$

$$\Delta HES_i = HES_{it} - HES_{t-1} \tag{13}$$

$$HEVR = P \times \Delta HES_i \tag{14}$$

where P is the rate of reverse conversion of ecosystem services; ΔS is the area of reverse conversion of ecosystem services; S is the area of the region; t and t-1 denote two neighboring different moments; ΔHES_i is the amount of risky loss; $HEVR$ is the ecological risk index, and the larger the value of which, the higher the ecological risk.

3. Results

3.1. Relationship between HESs and land use

3.1.1. HESs in 2000–2030

The inter-annual changes of HESs in the study area showed an increasing first and then decreasing trend. It was consistent with the rainfall pattern but showed a more extensive amplitude of change (Table 2). In 2010, the HESs reached the maximum. The average HESs amounts were 1350.52 mm, 1246.07 mm, and 1659.62 t/hm^2, respectively. In 20 years, from 2000 to 2020, the HESs showed an overall upward trend, during which the total water yield increased by 13.45 %, the total water conservation increased by 10.59 %, and the total soil conservation increased by 12.56 %. The most significant change occurred between 2005 and 2010, when water yield rose by 43.71 %, water conservation by 44.75 %, and soil conservation by 31.54 %. The main reason for these changes were the significant interannual differences in precipitation in the study area. HESs are greatly affected by rainfall.

Calculation of the global Moran index for the five periods from 2000 to 2020 showed that the overall aggregation of HESs in the study area increased, with a solid aggregation of water yield (Fig. 2b) and water conservation (Fig. 2a) and a relatively weak aggregation of soil conservation (Fig. 2c).

We used ArcGIS 10.2 to extract the 2020 raster data of a 15 km × 15 km fishing net and obtained 719 points. We chose the two most relevant factors affecting water yield and water conservation, that is, precipitation and evapotranspiration, and the two most relevant factors affecting soil retention, that is, elevation and slope, for correlation analyses. The correlation between water yield and water conservation (Fig. 3a) was robust for precipitation but weak for evapotranspiration (Fig. 3b). In addition, the correlation between soil conservation and slope was robust ($R^2 = 0.56$), but the correlation between soil conservation and DEM was weak ($R^2 = 0.72$) (Fig. 3c).

The spatial distribution of high-value water yield and water conservation areas in the basin showed a trend for a south to north shift, similar to the spatial distribution of rainfall each year (Fig. 4).

From 2000 to 2005, low-value water yields of 0–300 mm were mainly concentrated in the Poyang Lake area, those of 300–600 mm were primarily distributed in the northwestern and southwestern regions, and higher water yield areas were mainly found in the eastern part of the basin (Fig. 4a). Over time, from 2010 to 2020, the distribution of low water yield zones (0–300 mm) in the study area became more dispersed, especially in the urban built-up areas and around the rivers. This was accompanied by significantly less low-value zones in the lake area compared to 2000 and 2005. The low-value area of 300–900 mm was primarily concentrated in the Poyang Lake area and the southern part of the study area, whereas that of 1200–1500 mm was mainly distributed in the central and northeastern parts of the study area. The spatial distribution of water conservation was consistent with the distribution of water yield (Fig. 4b). With inter-annual changes, the low water conservation value in the north and west is becoming gradually apparent, and the high-value area in the study area is steadily shifting from the central and south to the northeastern region. The clustering of high and low values shows an overall trend of aggravation. In terms of soil conservation, the distribution changed little from 2000 to 2020. The areas with 0–1000 t were mainly concentrated in the watershed and unused land areas, while the regions with 1000–1500 t were mainly distributed in the plains around the watersheds (Fig. 4c). These are primarily areas with a large amount of cultivated land, resulting in a relatively low level of soil conservation. The high values were mainly found at the boundaries of the watersheds and in areas of high elevation. These areas are primarily forested, and the lush vegetation is responsible for the increased soil conservation capacity.

Table 2
HESs in Jiangxi province, 2000–2020.

Year	Average water yield (mm)	Total water yield (× 10^{8}m^3)	Average water conservation (mm)	Total water conservation (× 10^{8}m^3)	Average soil conservation (t/hm^2)	Total soil conservation (× 10^{8}t)
2000	885.75	1478.73	814.74	1351.3	903.98	150.45
2005	939.77	1568.93	863.45	1431.7	1261.74	209.53
2010	1350.52	2254.68	1246.07	2066.1	1659.65	276.22
2015	1154.89	1928.07	1080.68	1791.8	1428.67	237.78
2020	1003.43	1677.64	909.76	1494.4	1026.28	169.35

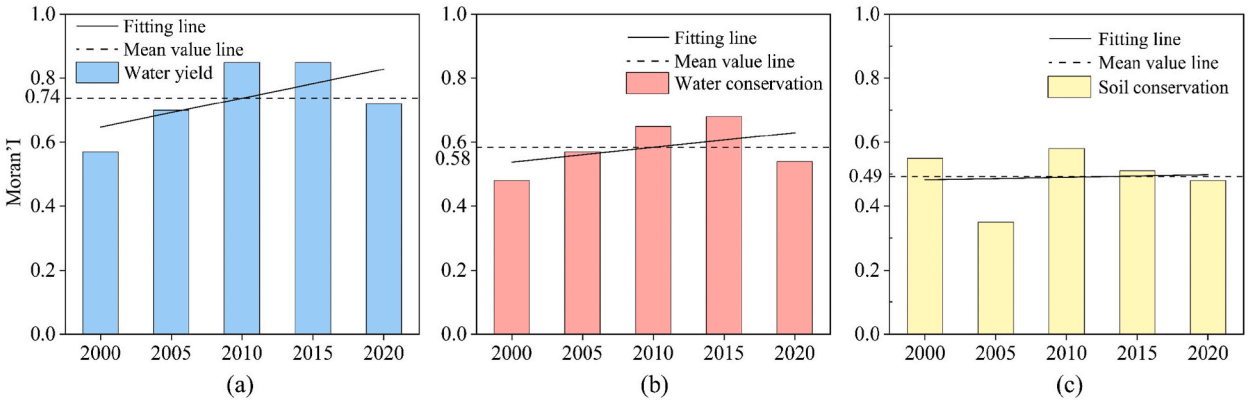

Fig. 2. Changes in the Moran index.

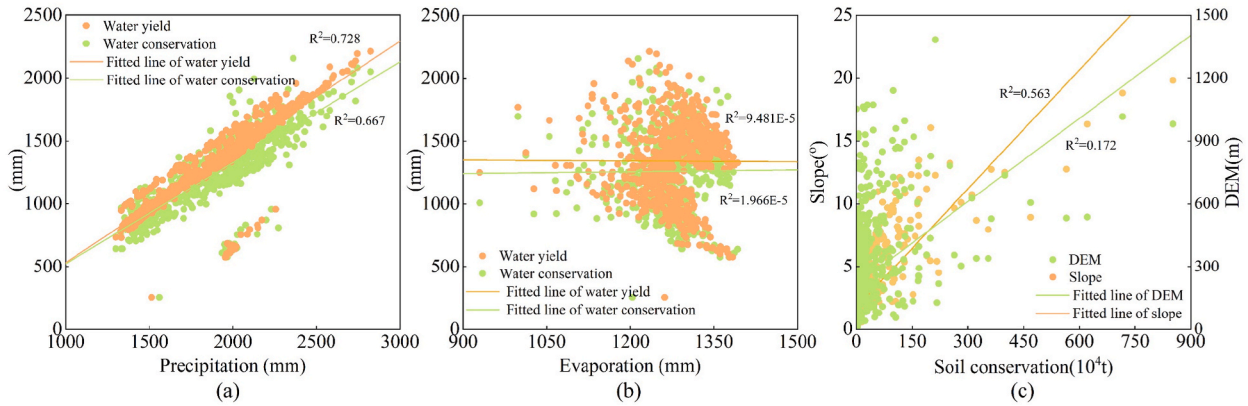

Fig. 3. Scatterplot of HESs in 2020.

3.1.2. Relationship between HESs and land use

The large difference in area between land use types resulted in too large a difference in HESs. Logarithmic transformed data were, therefore, used for comparative analyses. The total water yield of building land showed a yearly trend. For the other land types, the water yield showed a trend of increasing first and then decreasing, consistent with rainfall changes (Fig. 5a). The most significant water yield was found in forest land, followed by cultivated land. This was mainly because the forest and cultivated land areas accounted for a huge proportion of the study area. The average water yield of different land use types all showed an increasing and decreasing trend. Among them, building land had the highest water yield of 1081.74 mm, followed by cultivated land. The lowest was found for unused land, with only 995.28 mm (Fig. 5b).

The water conservation of building land and unused land in the study area was 0, indicating that the amount of runoff from the same amount of rainfall was more significant than or equal to the amount of water yield under the selected runoff coefficient (Fig. 5c). The water conservation of the other lands increased and then decreased. The forest land had the highest water conservation of 990.48 mm, followed by cultivated land (Fig. 5d).

The soil conservation of cultivated land, forest land, grassland, and water in the study area increased from 2000 to 2010 and decreased from 2010 to 2020, the same trend observed for land use area change (Fig. 5e). Between 2000 and 2020, the average soil conservation of unused land showed a fluctuating trend of decreasing and then increasing and decreasing, while the other land types showed a trend of increasing and then decreasing (Fig. 5f). Overall, the average soil conservation of forest land was the largest, followed by grassland, suggesting that, among all land types, forest land and grasslands were more advantageous in terms of soil conservation. During the period 2000–2020, cultivated land, forest land, grassland, and unused land decreased, while building land increased. In other words, the decrease was mainly found for the land types with high soil conservation. An increase in building land had a particularly negative effect on soil conservation, and this affected the overall level of soil conservation.

3.2. Land use and HESs under different strategies

3.2.1. Land use simulation

The land use map of 2015 was simulated based on the land use of 2005 and 2010. DEM, slope, aspect, national highway, highway,

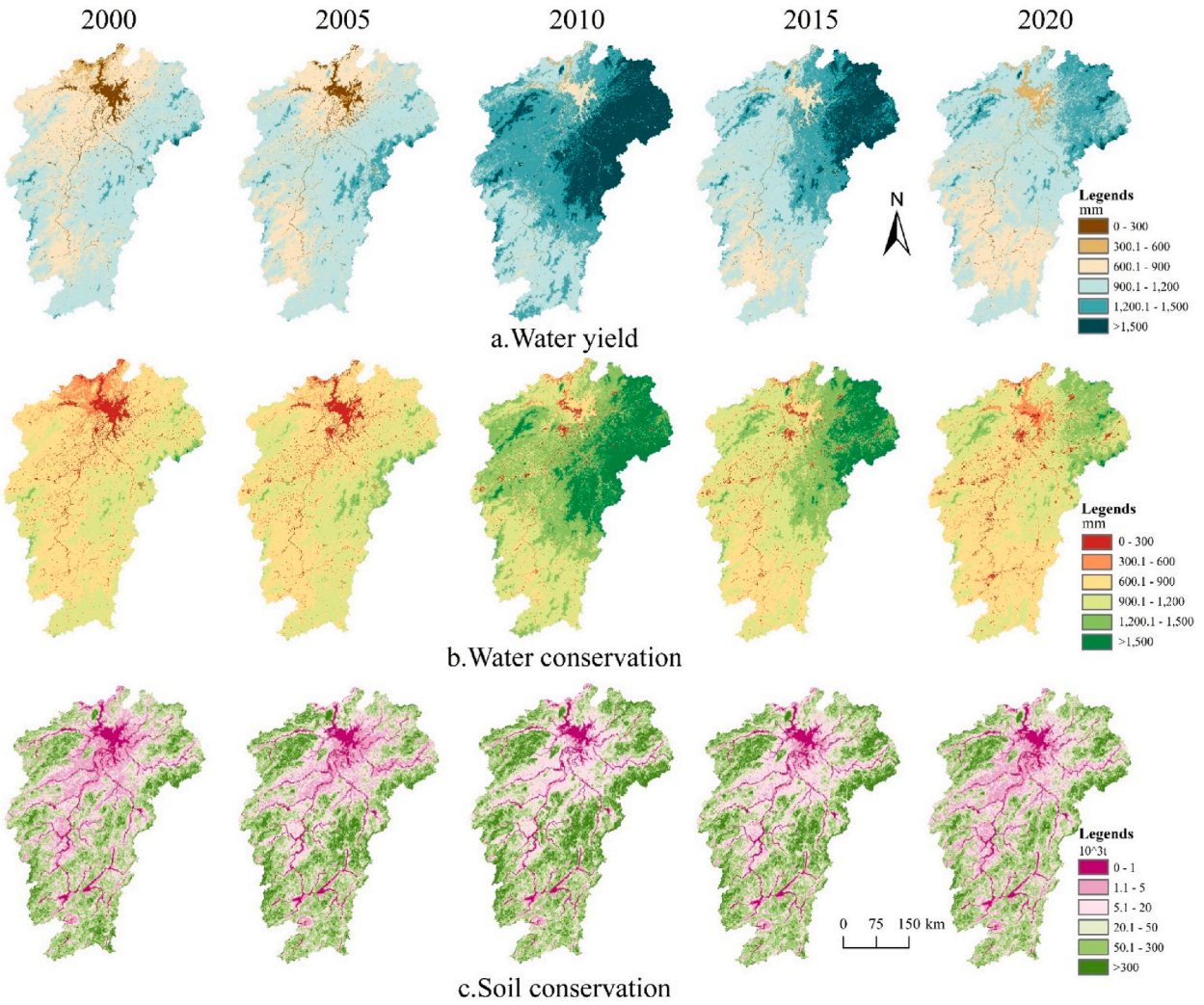

Fig. 4. Spatial distribution of HESs in Jiangxi Province, 2000–2020.

railroad, river, and population data were used as driving factors, and watersheds and ecological protection zones as restriction zones. After consistency testing with the actual land use map, the kappa coefficient was calculated as 0.92. This value is accurate and can be used for subsequent research. After simulation, the land use for 2030 was obtained under three different development strategies (Fig. 6a).

Under the three development strategies, the land use of the study area was dominated by forest land and cropland (Fig. 6b). Cropland had the same share of 26.25 % under both the natural development strategy and the ecological protection (EP) strategy. This slightly decreased for the urban expansion strategy, which was 25.89 %. Forest land had the largest share under EP, which was 61.50 %, and the smallest under the urban expansion strategy, which was 59.83 %. Grassland had the largest share under the natural development strategy, which was 4.90 %, and the smallest in the urban expansion strategy, which was 59.83 %. Grassland had the largest share under the natural development strategy, which was 4.90 % for EP and 4.26 % for the ecological development strategy. The share of water area was similar among strategies. The built-up land had the largest share of 4.78 % under the urban expansion strategy and the smallest share of 3.32 % under the ecological development strategy. There was no change in the share of unused land, both of which was 0.36 %.

A comparison of land use changes in 2030 showed that cropland, forested land, and watersheds would all decrease under the three future development strategies (Fig. 6c). In particular, all three reductions would reach the maximum under the nature strategy and the minimum under EP. Grassland, on the other hand, will rise under the nature strategy and the construction expansion strategy, mainly due to the degradation of forest land to grassland. Construction land will continue to grow under all three strategies. At the same time, construction land will significantly change under the urban expansion strategy, increasing by 243,800 km^2, or 4.50 %, but it will only increase by 2800 km^2 under EP.

In summary, according to the land use changes simulated under different strategies, different land planning needs can be regulated.

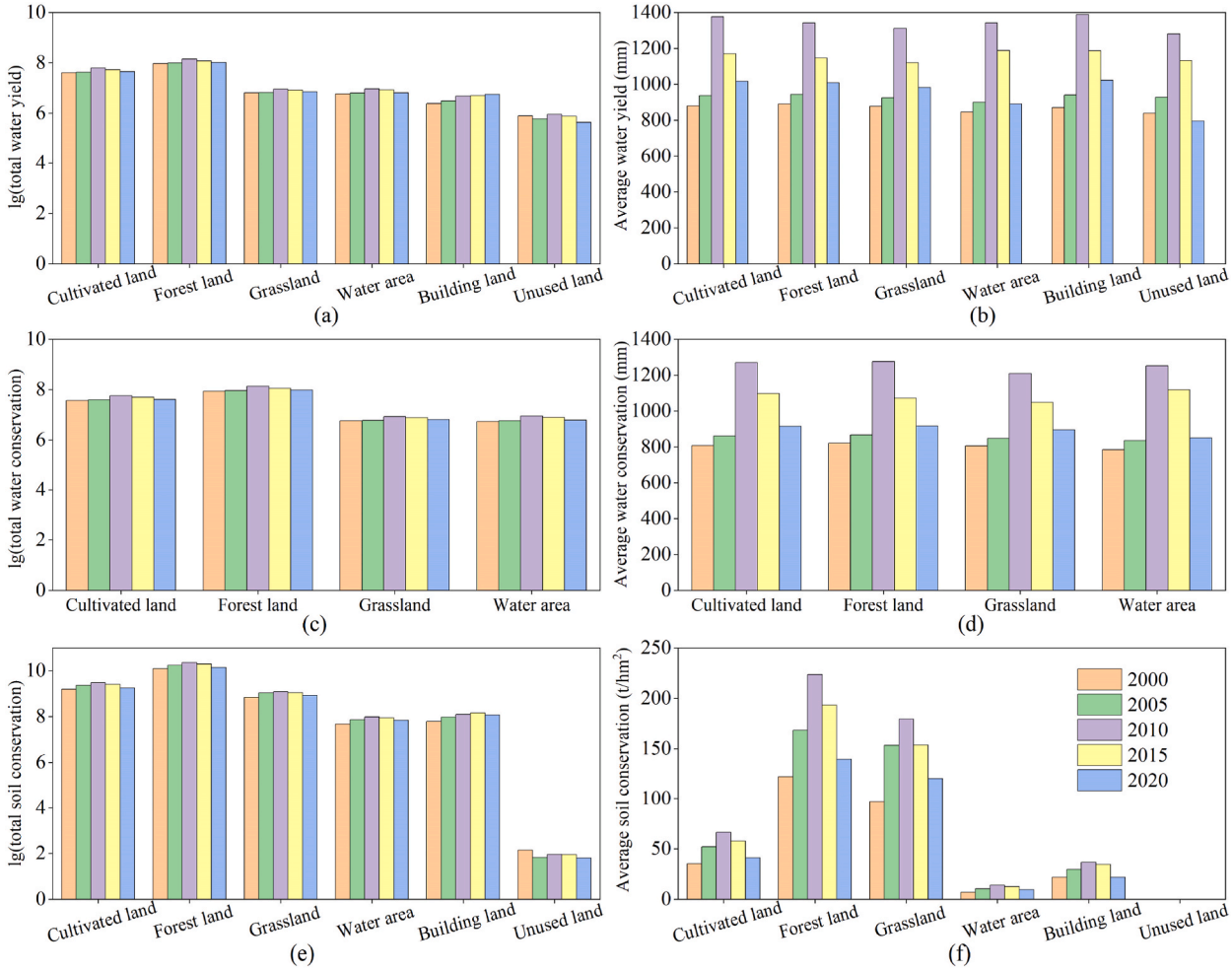

Fig. 5. HESs from different land uses in Jiangxi Province, 2000–2020.

The area of construction land in Poyang Lake Basin expanded to different degrees, and the cultivated land and ecological type forest land were reduced and destroyed to different degrees. In the future, for the sustainable development of land resources and protection of the ecological environment in Poyang Lake Basin, land resources should be rationally allocated, the intensity of land use should be improved, and the ecological environment should be considered part of the economic development.

3.2.2. HESs under different strategies

According to the predictions, with advances in urbanization, all HESs in the study area are expected to experience some degree of decline by 2030 (Table 3). Nevertheless, there were significant variations in the HESs of the basin across different strategies. In terms of water yield, the most substantial decrease was observed for urban sprawl (US), with a total reduction of 2.51×10^8 m^3 and a change rate of −0.15 %. EP, however, resulted in a total water yield decrease of 1.22×10^8 m^3 and a change rate of −0.07 %. This suggests that urban expansion leads to an increase in building land, which in turn enhances the water yield in the watershed. Under the natural development strategy, the water conservation in the watershed decreased by 27.72×10^8 m^3 compared to 2020, with a change rate of −1.84 %. The most substantial decrease was observed for US, with a total water conservation decrease of 38.51×10^8 m^3 and a change rate of −2.55 %. A smaller decrease occurred for EP, with the total water conservation decreasing by 14.01×10^8 m^3 and resulting in a decline of −2.55 %. EP showed a minor reduction of 14.01×10^8 m^3. This was primarily due to the implementation of ecological protection measures, which resulted in the improvement of forest land and grassland, thereby slowing down the expansion of building land and enhancing water conservation. The total soil conservation values remained identical under both the natural development and urban expansion strategies, suggesting that the expansion of towns and cities had a minimal impact on soil conservation. Conversely, EP had a positive influence on soil conservation, with only a −2.66 % decrease. In contrast, under the natural development and urban expansion strategies, soil conservation decreased by −2.73 %.

There was little difference in the spatial distribution of HESs among the three strategies. The distribution of water yield and conservation was relatively consistent, with the characteristics “high all around, low in the middle, and gradually increasing from

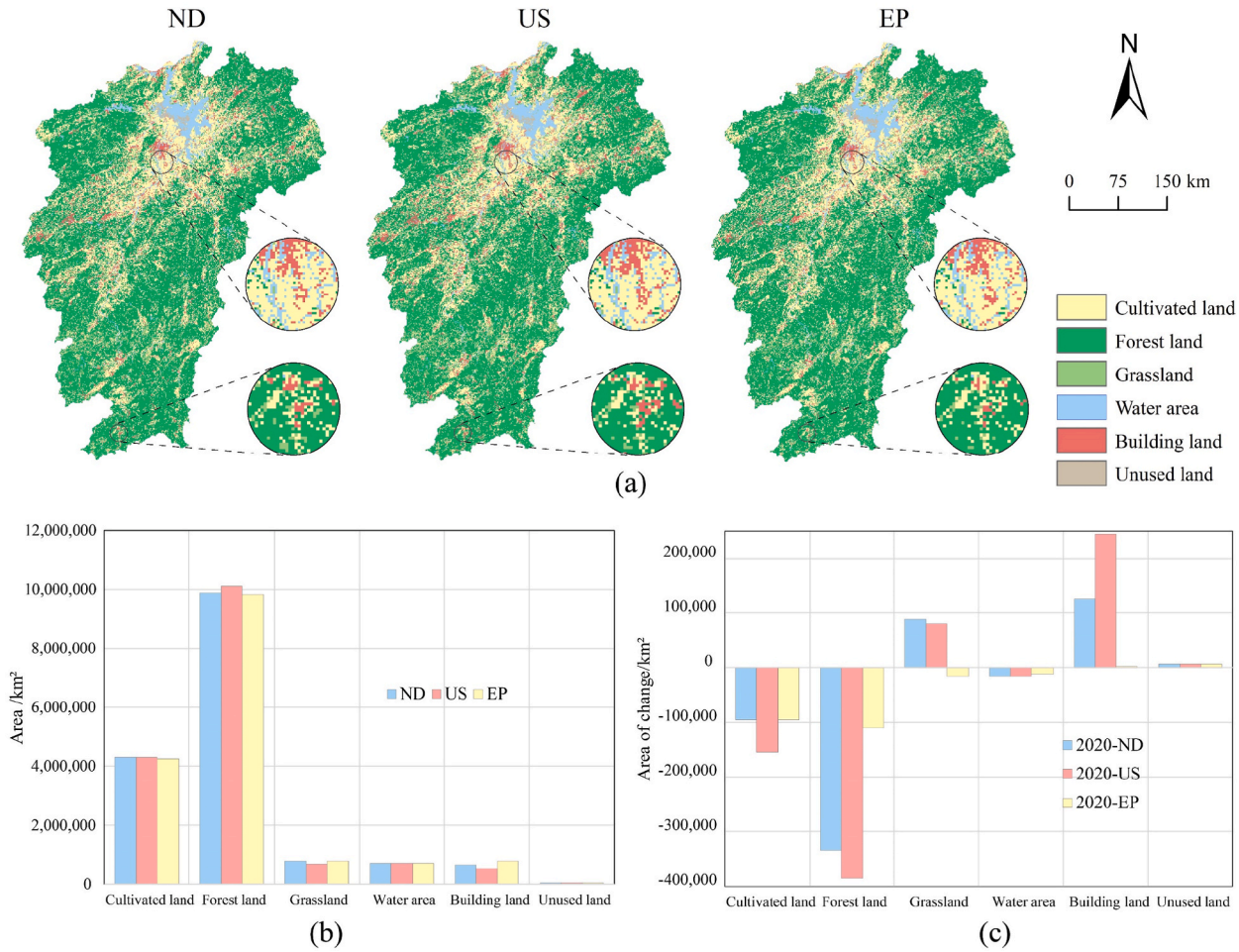

Fig. 6. Changes in land use area under different strategies.

Table 3
HESs under different strategies in 2020 and 2030.

Strategies	Total water yield ($\times 10^8 m^3$)	Total water conservation ($\times 10^8 m^3$)	Total soil conservation ($\times 10^8 t$)
2020	1677.01	1509.4	169.35
ND	1675.22	1481.7	164.73
US	1674.50	1470.9	164.73
EP	1675.79	1495.3	164.84

south to north (Fig. 7a) (Fig. 7b)." In contrast, the high soil conservation value was still concentrated in the hilly areas around the watershed, which tend to have higher elevation and better vegetation cover, and are less affected by human activities (Fig. 7c). Areas with low soil conservation are mainly concentrated around rivers and lakes. Because of the scouring of rivers, these areas are less resistant to soil erosion. In addition, because of their fertile soils, plains are developed into cultivated land for the cultivation of food crops, resulting in a relatively poor soil conservation.

3.3. HEVR of HESs under different strategies

The natural breakpoint method was used to categorize the ecological risks into five levels, with higher levels indicating greater ecological risk. There was a significant disparity in the distribution of risk levels across the study area, under various strategies (Table 4). Generally, the highest proportion of risk fell within level 1, exceeding 12.63 % for all three strategies, while the lowest percentage corresponded to level 4 consistently hovering around 0.30 %. Comparing the three strategies, the lowest rate of risk was observed for EP, followed by the natural development strategy, and the highest percentage was observed for US. It is worth noting that, for US, the proportions of all risk levels were the largest, except for level 4, suggesting that urban expansion was the main factor

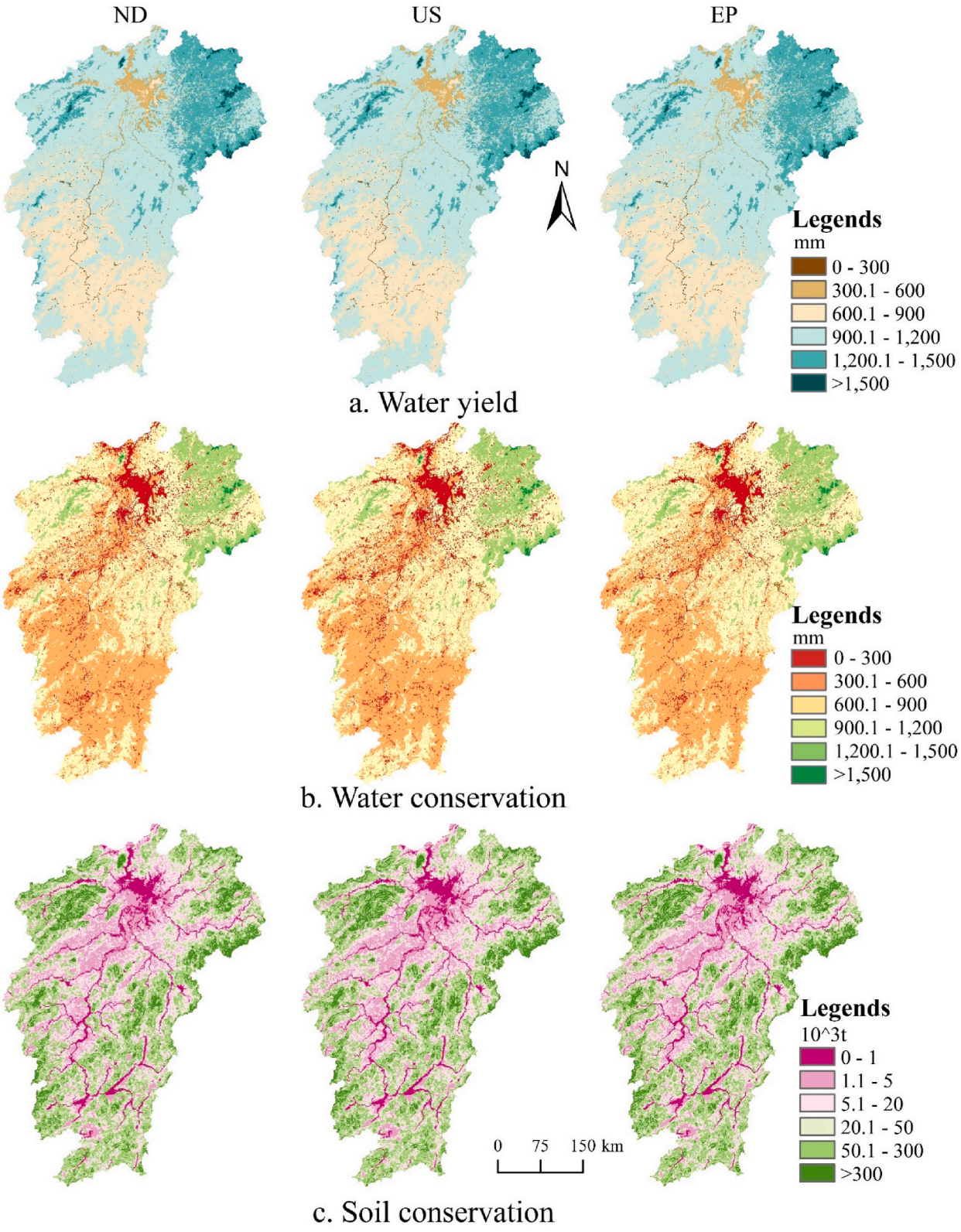

Fig. 7. Spatial distribution of HESs under different land use strategies.

Table 4
Percentage of each risk level.

Strategies	Level 1	Level 2	Level 3	Level 4	Level 5	Sum
ND	13.69 %	1.74 %	0.84 %	0.30 %	2.63 %	19.19 %
US	14.39 %	1.65 %	0.88 %	0.29 %	2.58 %	19.79 %
EP	12.63 %	1.87 %	0.75 %	0.30 %	2.66 %	18.21 %

contributing to the increase in ecological risk. Conversely, for EP, the constraints imposed by the ecological protection zone and the curtailment of building-land expansion have enhanced the ecological environment and diminished ecological risk in the study area.

Regarding spatial distribution of risk areas, all three strategies exhibited a "low in the south and high in the north" pattern. High-risk areas were predominantly concentrated in and around urban areas, while medium-risk areas were primarily situated along riverbanks. There was no substantial variation in the distribution of risk levels among the three strategies (Fig. 8).

Under the three land use strategies, only a few plots changed, resulting in little spatial difference in HESs. Nevertheless, significant differences in risk levels were observed at the municipal scale. As observed in Fig. 9, under varying land use strategies, Ganzhou, Shangrao, Ji'an, Nanchang, and Jiujiang exhibited relatively substantial and prominent proportions of risk areas.

Under the natural development strategy, Ganzhou had the highest ecological risks, followed by Ji'an and Pingxiang. Among these cities, under the natural development strategy, Ganzhou had the highest distribution of risk, that is, level 5, at 18.71 %, followed by Ji'an at 14.67 %. Risk level 4 was most prevalent in Yingtan, accounting for 41.49 %, followed closely by Ganzhou at 40.73 %. Risk level 3 was most common in Yichun, constituting 22.16 %, followed by Jiujiang at 22.81 %. Risk level 2 dominated in Shangrao, accounting for 29.68 %, followed by Jiujiang at 22.81 %. Risk level 1, the lowest, was most prevalent in Ganzhou at 23.90 %, followed by Fuzhou at 12.59 %. Under US, Ganzhou had the highest distribution of risk, that is, level 5, at 19.40 %, followed by Ji'an at 15.34 %. Risk level 4 was most prevalent in Ji'an, accounting for 45.11 %, followed by Ganzhou at 41.28 %. Risk level 3 was most common in Ji'an, constituting 22.38 %, followed by Nanchang at 19.13 %. Risk level 2 dominated in Shangrao, accounting for 30.88 %, followed by Jiujiang at 23.11 %. Risk level 1 was most widespread in Ganzhou, with 24.09 %, followed by Ji'an at 17.36 %. In summary, under US, Ganzhou and Ji'an continued to exhibit the highest distribution of risk, and Pingxiang and Xinyu the lowest risk proportion. Under the eco-protection strategy, level 5 and level 4 risks were most widely distributed in Ganzhou, followed by Ji'an. Level 3 risks were most widely distributed in Ji'an, with 22.27 %, followed by Yichun, with 21.53 %. Level 2 risks had the largest share in Shangrao, followed by Jiujiang, with 27.96 % and 22.57 %, respectively. Level 1 risks were most widely distributed in Ganzhou, followed by Ji'an, with 24.12 % and 18.06 %. Comparing the ND and US, the distribution of risk levels in each decreased under the ecological strategy.

The risk of reverse transformation of HESs in the watershed differed under different land use development strategies. Comparing the three strategies, the ecological risk was better under EP than under the natural development and urban expansion strategies, suggesting that natural protection measures favor the development of HESs in the study area. Also, in the different land-use development strategies, ecological risk occurs in Ganzhou, Ji'an, Shangrao, and Jiujiang. Future land use planning and development programs should include the ecosystem services of these regions to ensure that development and ecological protection go hand in hand.

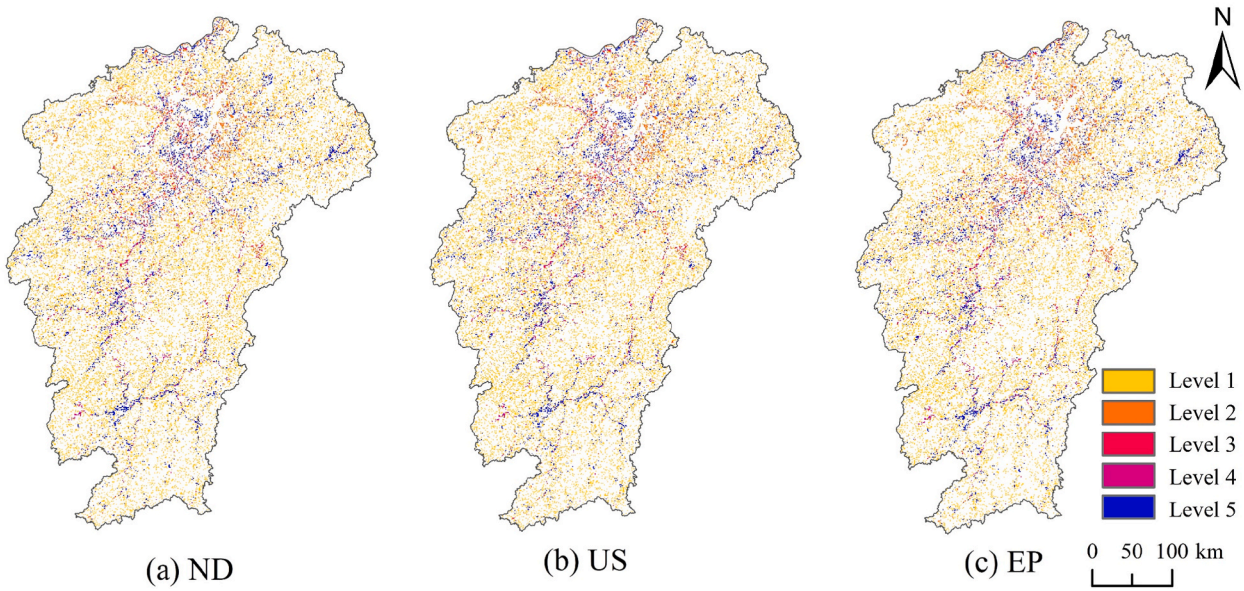

Fig. 8. Distribution of ecological risk levels for different land use strategies.

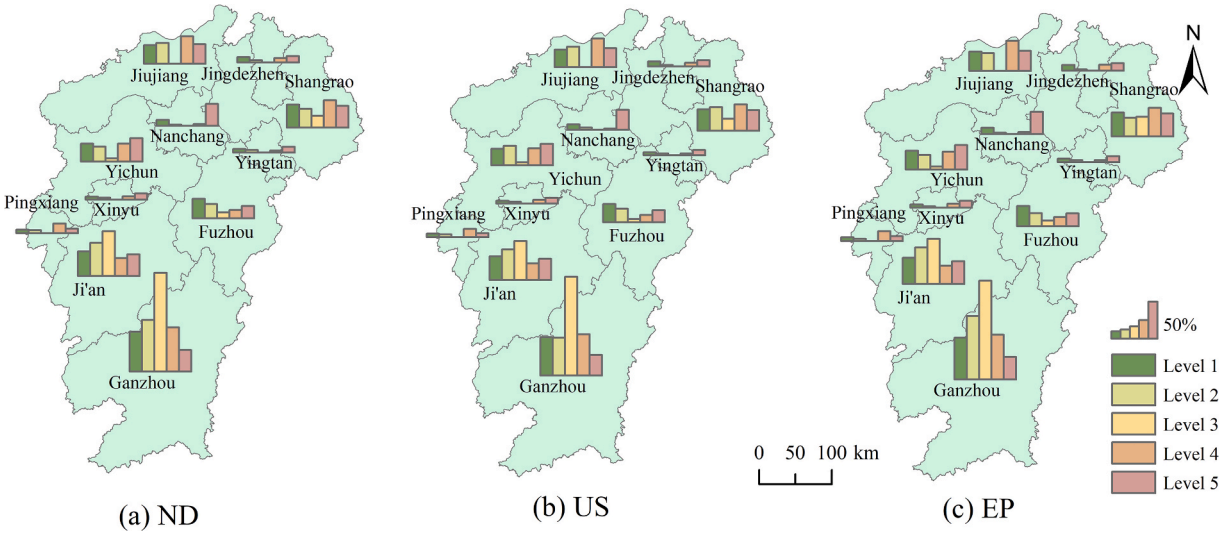

Fig. 9. Distribution of ecological risks at different levels in different cities.

4. Discussion

4.1. Relationship between HESs and land use

The present study showed that the HESs in the study area were robust but exhibited significant spatial and temporal variations. Despite abundant precipitation, these variations were primarily attributed to spatial and temporal disparities within the study area [47]. Water yield and conservation gradually shifted from the south to the north. Conversely, soil conservation exhibited remarkable stability, demonstrating a "high in the surrounding areas and low in the central region" pattern over the last two decades. It was evident that the HESs exhibited significant variations across different land types. Notably, building land showed the highest water yield among the land types. In contrast, forest land and grassland demonstrated substantial advantages in terms of water conservation and soil conservation, aligning with the findings of Zou et al. [48] and Zhang et al. [49]. This may be primarily attributed to the fact that forest land and grasslands typically feature stable vegetation cover and extensive plant root systems, which promote soil conservation and structural stability. Trees and grasslands are effective in reducing the exposed soil surface area, mitigating the impact of rainfall on the soil, and slowing down water flow rates, thereby reducing the risk of soil erosion [50]. Conversely, vegetation can raise water demand, consequently reducing water yield. Accelerated urbanization typically coincides with expanding building land, increasing water yield in urban areas [51]. The expansion of building land has a counteractive impact on water conservation and soil conservation, primarily because water conservation relies on the water interception cap of vegetation-covered areas such as forests and grasslands. Despite the particular influence of reduced permeability from land hardening on soil conservation, our findings suggest that soil conservation are most robust in areas with abundant vegetation growth, particularly in mountainous and hilly regions, exhibiting a positive correlation with site elevation. Furthermore, land use minimally affects water yield and water conservation but significantly influences soil conservation.

4.2. Land use and HESs under different strategies

Land-use simulations were performed by incorporating multiple driving influences, and favorable results were obtained. By changing the probability of land use transfer, a land use map and HESs under three strategies were simulated. The most significant change under the different strategies was found for construction land, mainly because of the undeniable short-term demand for construction land. Construction land is mainly found in plains with lower slopes [52], meaning that most of it encroaches on the cultivated land [53]. At the same time, under the implementation of existing policies such as "returning cultivated land to the forest" and "returning cultivated land to grass" in China, deforestation of hilly areas is limited. This is supported by the predictions under the three strategies. The differences between HESs under different land use strategies were insignificant, mainly because HESs are also affected by precipitation, evapotranspiration, and slope. Since these factors are highly uncertain, the effects of land use change on HESs were explored by controlling for these factors. The differences in the impact of different land uses on water yield and conservation were found to be minor. The differences in the effects of different land use types on soil conservation were, however, significant, and forested land and grassland remained the key land types for preventing soil erosion. This is consistent with the results of Du et al. [54] and Zhao et al. [55]. HESs declined to some extent under different land use strategies. The impact of land use on water yield and water conservation was minimal, and the effect on soil conservation was clear. Human activities are characterized by land use change. In the short term, therefore, controlling such land use change through ecological protection policies will have a positive effect on soil conservation. The response of water yield and water conservation to land use was expected to be stronger, although in the present

study, construction land was found to have the highest water yield. This is because the calculation of evapotranspiration included primarily the depth of the vegetation root system and the chosen evapotranspiration coefficient. In addition, the building land showed the lowest vegetative root depth and evapotranspiration, resulting in the highest water yield with identical precipitation amounts.

4.3. HEVR and policy recommendations

Based on the composite index of ecosystem services calculated, after normalization, under each land use development strategy, the risk level distribution of ecosystem service reverse transformation induced by land use changes was obtained by superimposing the three strategies on the 2020 data. The differences in the distribution of risk levels under different strategies were relatively small, but all of them were dominated by risk level 1. Comparing the three strategies, the risk level under ecological protection accounted for the least, followed by the natural development strategy. US accounted for the most. This suggests that environmental protection measures benefit ecosystem services in the watershed, while US increases ecological risks in the watershed. Under different land use development strategies, most risk areas in the watershed were mainly distributed in Ganzhou, Ji'an, Shangrao, and Jiujiang. For subsequent developmental projects, therefore, the ecological protection of these regions should be strengthened, and urban land use should be rationally planned.

From the perspective of changes in HESs and ecosystem service risk zoning, the study area, as an essential grain production base in the middle and lower reaches of the Yangtze River, is China's "ecological civilization demonstration area." Decision-making departments should, therefore, take HESs of the study area into account in land-use management and policy formulation. First, the scale of cultivated land should be controlled to ensure food production, and control should be strengthened in areas with high water ecological risk. Second, as rivers and lakes surround the study area, the HESs of the study area should be considered.

4.4. Advantages and limitations of the study

In this study, HESs were simulated under various strategies using predicted land use patterns. Simultaneously, the effects of different land types on ecosystem services were quantified. The obtained results are applicable and hold significance for future land use policy planning in the region. To minimize uncertainty arising from abrupt data changes, our study was based on data spanning five periods from the past 20 years. Ultimately, the ecosystem service risk situation was assessed for each regional prefecture. This assessment serves as a valuable reference for future ecological risk prevention efforts. Nevertheless, this paper has certain limitations. In terms of raster accuracy, for example, we used 1 km $\times$ 1 km raster data for calculations. In the future, higher-precision raster data should be employed to enhance the assessment.

5. Conclusion

The evolving patterns of HESs were examined in Jiangxi Province from 2000 to 2020, the impacts of each land type on HESs were quantified, and the strategies of ecosystem service risks for each municipality under various future land use strategies were analyzed. On the one hand, water yield and conservation exhibited spatial heterogeneity and were significantly influenced by rainfall. On the other hand, soil conservation exhibited a strong correlation between its primary distribution and elevation, with most high-value distribution areas located in forested regions like hills and mountains. Building land had a positive effect on water yield, but the effect is not significant; forest land, grassland, and cultivated land are conducive to soil conservation. The quantity of each HES declined under the three future strategies. Nonetheless, EP positively affected HESs, suggesting that environmental protection enhances HESs. Simultaneously, the expansion of building land threatened HESs. The ecological risk level in the study area was primarily categorized as level 1, with risk areas concentrated mainly in Ganzhou, Ji'an, Shangrao, and Jiujiang. The distribution of ecological risk areas remained consistent across different strategies. The comparison, however, highlights that environmental protection measures yield more significant benefits for HESs, while urban expansion heightens the risk to these services in the study area. The present study provides a reference for the prevention of ecological risks and the promotion of sustainable development in the region, as well as a direction for future ecosystem risk assessment.

Data availability statement

Data associated with the study has not been deposited into a publicly available repository and data will be made available on request.

CRediT authorship contribution statement

Chun Fu: Writing – review & editing, Supervision, Conceptualization. **Yezhong Liu:** Writing – original draft, Formal analysis, Data curation. **Fan Li:** Writing – original draft, Software, Methodology, Investigation. **Huimin Huang:** Visualization, Supervision. **Shuchen Zheng:** Visualization, Validation, Supervision.

Declaration of competing interest

The authors declare that they have no known competing financial interests or personal relationships that could have appeared to

influence the work reported in this paper.

Acknowledgements

Partial funding from the National Social Science Foundation of China (Approval No. 18BGL187) and the Science and Technology Program of Jiangxi Province, China (Approval No. 20213BAA10W43) is gratefully acknowledged.

References

[1] R. Costanza, R. d'Arge, R.d. Groot, et al., The value of the world's ecosystem services and natural capital, NATURE 387 (1997) 253–260, https://doi.org/10.1038/387253a0.
[2] G.C. Daily, Nature's Services. Societal Dependence on Natural Ecosystems, Island Press, Washington, DC, 1997.
[3] J. Cai, X. Wei, P. Jiang, et al., Ecosystem Service Trade-Off Synergy Strength and Spatial Pattern Optimization Based on Bayesian Network: A Case Study of Fenhe River Basin, Environmental Science, 2023, pp. 1–17, https://doi.org/10.13227/j.hjkx.202305204.
[4] C. Chen, Z. Chen, Z. Yao, Current situation of water resources in China and countermeasures, Adv. Sci. Technol. Water Resour. 26 (1) (2006) 1–5.
[5] MA, Ecosystems and Human Well-Being: Opportunities and Challenges for Business and Industry, World Resources Institute, Washington, DC, 2005.
[6] J. Xia, J. Zhai, C. Zhan, Some Reflections on the research and of development water resources in China, Advance in Earth Sciences 26 (9) (2011) 905–915.
[7] P. Meyfroidt, A. de Bremond, C.M. Ryan, et al., Ten facts about land systems for sustainability, Proc. Natl. Acad. Sci. U.S.A. 119 (7) (2022), https://doi.org/10.1073/pnas.2109217118.
[8] S.S. Hasan, L. Zhen, M.G. Miah, et al., Impact of Land Use Change on Ecosystem Services: A Review, vol. 34, Environmental Development, 2020, https://doi.org/10.1016/j.envdev.2020.100527.
[9] S. Sannigrahi, S. Bhatt, S. Rahmat, et al., Estimating global ecosystem service values and its response to land surface dynamics during 1995-2015, J. Environ. Manag. 223 (2018) 115–131, https://doi.org/10.1016/j.jenvman.2018.05.091.
[10] M. Kindu, T. Schneider, D. Teketay, et al., Changes of ecosystem service values in response to land use/land cover dynamics in Munessa-Shashemene landscape of the Ethiopian highlands, Sci. Total Environ. 547 (2016) 137–147, https://doi.org/10.1016/j.scitotenv.2015.12.127.
[11] J. Ning, Q. Shao, Temporal and spatial characteristics of land use and ecosystem services in the Loess Plateau, Journal of Agro-Environment Science 39 (4) (2020) 774–785, https://doi.org/10.11654/jaes.2020-0112.
[12] W. Zhang, J. Xie, Z. Liu, et al., Assessment of the ecosystem service value change in Ningxia in 2000-2020, J. Desert Res. 43 (4) (2023) 1–11, https://doi.org/10.7522/j.issn.1000-694X.2023.00022.
[13] Z.a. Chen, Z. Liu, L. Zhang, et al., Multi-scenario simulation of LUCC and Spatio-temporal evolution and prediction of Habitat quality in Nanchang city, Trans. Chin. Soc. Agric. Mach. 54 (5) (2023) 170–180.
[14] X. Xie, X. Liin, Y. Wang, et al., Multi-scenario simulation of land Use in Nanchuan district of chongqing based on PLUS model, Journal of Changjiang River Scientific Research Institute 40 (6) (2023) 86–92+113, https://doi.org/10.11988/ckyyb.20221227.
[15] Z. Wang, B. Wang, Y. Zhang, et al., Dynamic simulation of multi-scenario land use change and carbon storage assessment in Hohhot city based on PLUS-InVEST model, J. Agric. Resour. Econ. (2023) 1–18, https://doi.org/10.13254/j.jare.2023.0249.
[16] P. Zou, F. Xu, Ecological security pattern construction and landscape ecological risk prediction by coupling ERI-MCR-PLUS model: a case study of Saihanwula National Nature Reserve, Acta Ecol. Sin. (23) (2023) 1–13, https://doi.org/10.5846/stxb202211213360.
[17] X. Liang, Q. Guan, K.C. Clarke, et al., Understanding the drivers of sustainable land expansion using a patch-generating land use simulation (PLUS) model: a case study in Wuhan, China, Comput. Environ. Urban Syst. 85 (2021), https://doi.org/10.1016/j.compenvurbsys.2020.101569.
[18] N. Pan, Q. Guan, Q. Wang, et al., Spatial differentiation and driving mechanisms in ecosystem service value of arid region:A case study in the middle and lower reaches of shule River Basin, NW China, J. Clean. Prod. 319 (2021), https://doi.org/10.1016/j.jclepro.2021.128718.
[19] M. Marques, R.F. Bangash, V. Kumar, et al., The impact of climate change on water provision under a low flow regime: a case study of the ecosystems services in the Francoli river basin, J. Hazard Mater. 263 (2013) 224–232, https://doi.org/10.1016/j.jhazmat.2013.07.049.
[20] F. Wang, Q. Tao, X. Cheng, et al., Influence of landscape pattern change on water ecosystem service in rapidly urbanization areas, J. Soil Water Conserv. 37 (1) (2023) 159–167, https://doi.org/10.13870/j.cnki.stbcxb.2023.01.022.
[21] K.J. Bagstad, J.M. Reed, D.J. Semmens, et al., Linking biophysical models and public preferences for ecosystem service assessments: a case study for the Southern Rocky Mountains, Reg. Environ. Change 16 (7) (2016) 2005–2018, https://doi.org/10.1007/s10113-015-0756-7.
[22] S. Huo, L. Huang, L. Yan, Valuation of cultural ecosystem services based on SolVES: a case study of the south ecological park in Wuyi County,Zhejiang province, Acta Ecol. Sin. 38 (10) (2018) 3682–3691, https://doi.org/10.5846/stxb201704110624.
[23] R. Boumans, J. Roman, I. Altman, et al., The multiscale integrated model of ecosystem services (MIMES): simulating the interactions of coupled human and natural systems, Ecosyst. Serv. 12 (2015) 30–41, https://doi.org/10.1016/j.ecoser.2015.01.004.
[24] M. Liu, J. Zhong, B. Wang, et al., Spatiotemporal change and driving factor analysis of the Qinghai Lake Basin based on InVEST model, Sci. Geogr. Sin. 43 (3) (2023) 411–422, https://doi.org/10.13249/j.cnki.sgs.2023.03.004.
[25] A.K. Mashizi, M. Sharafatmandrad, Investigating tradeoffs between supply, use and demand of ecosystem services and their effective drivers for sustainable environmental management, J. Environ. Manag. 289 (2021), https://doi.org/10.1016/j.jenvman.2021.112534.
[26] Y. Wang, A. Ye, D. Peng, et al., Spatiotemporal variations in water conservation function of the Tibetan Plateau under climate change based on InVEST model, Journal of Hydrology-Regional Studies 41 (2022), https://doi.org/10.1016/j.ejrh.2022.101064.
[27] Q. Duan, J. Xia, C. Miao, et al., The uncertainty in climate change projections by global climate models, Nat. Mag. 38 (3) (2016) 182–188, https://doi.org/10.3969/j.issn.0253-9608.2016.03.004.
[28] J. Wang, Y. Dun, A review on the effects of land use change on ecosystem services, Resour. Environ. Yangtze Basin 24 (5) (2015) 798–808, https://doi.org/10.11870/ejlyzyyhj201505012.
[29] People's Government of Jiangxi province, C. Introduction to Jiangxi [cited 2023 September 6, 2023]; Available from: http://www.jiangxi.gov.cn/col/col471/index.html, 2022.
[30] W. Zhou, A Study on Available Water Capacity of Main Soil Types in China Based on Geographic Information System, Nanjing Agricultural University, 2003.
[31] R. Sharp, R. Chaplin-Kramer, S. Wood, et al., InVEST 3.13.0.post11+ug.Gfa34215 User's Guide, 2022 [cited 2023 April 29]; Available from: https://storage.googleapis.com/releases.naturalcapitalproject.org/invest-userguide/latest/zh/index.html#.
[32] C. Liu, Spatial-temporal Evolution of Supply-demand of Water Supply and Water Purification Service in Taihu Basin, Nanjing Agricultural University, 2019.
[33] Y. Cao, L. Xu, H. Fan, et al., Impact of climate change and human activities on the changes of ecological flow indicators in the Lake Poyang Basin since 1960s, Hupo Kexue 34 (1) (2022) 232–246, https://doi.org/10.18307/2022.0119.
[34] H.-w. Guo, X.-y. Sun, L. Li-shu, et al., Response of water yield function of ecosystem to land use change in Nansi Lake Basin based on CLUE-S model and InVEST model, Yingyong Shengtai Xuebao 27 (9) (2016) 2899–2906, https://doi.org/10.13287/j.1001-9332.201609.039.
[35] W. Zhang, J. Fu, Rainfall erosivity estimation under different rainfall amount, Resour. Sci. 25 (1) (2003) 35–41.
[36] J.R. Williams, The EPIC Model, 1995, pp. 909–1000.
[37] C. Gu, Y. Zhu, R. Li, et al., Change of the rainfall erosivity in Poyang Lake Basin and its influence on Suspended sediment load into the lake, J. Soil Water Conserv. 35 (6) (2021) 45–54, https://doi.org/10.13870/j.cnki.stbcxb.2021.06.007.
[38] J. Li, F. Sheng, S. Liu, et al., Variation of rainfall erosivity and its influencing factors in Jiuqushui Watershed,Southern Jiangxi province, J. Soil Water Conserv. 36 (4) (2022) 63–73, https://doi.org/10.13870/j.cnki.stbcxb.2022.04.009.

[39] China, M.o.E.a.E.o.t.P.s.R.O. And N.D.a.R.C.O. China. Guidelines for Delineating Ecological Protection Red Lines, 2017 [cited 2023 September 3, 2023]; Available from: https://www.mee.gov.cn/gkml/hbb/bgt/201707/t20170728_418679.htm.
[40] E. Rao, Z. Ouyang, X. Yu, et al., Spatial patterns and impacts of soil conservation service in China, Geomorphology 207 (2014) 64–70, https://doi.org/10.1016/j.geomorph.2013.10.027.
[41] K.G. Renard, G.R. Foster, G.A. Weesies, et al., Rusle - revised universal soil loss equation, J. Soil Water Conserv. 46 (1) (1991) 30–33.
[42] X. Pan, P. Shi, N. Wu, Ecological risk assessment and identification of priority areas for management and control based on the perspective of ecosystem services equilibrium: a case study of Lanzhou, Acta Sci. Circumstantiae 40 (2) (2020) 724–733, https://doi.org/10.13671/j.hjkxxb.2019.0437.
[43] M. Wang, Y. Ti, J. Wang, et al., Ecosystem services, trade-offs and synergy analysis in Tianjin under different land use scenarios, J. Beijing For. Univ. 44 (5) (2022) 77–85, https://doi.org/10.12171/j.1000-1522.20210008.
[44] S. Yang, H. Su, G. Zhao, Multi-scenario simulation of urban ecosystem service value based on PLUS model: a case study of Hanzhong city, J. Arid Land Resour. Environ. 36 (10) (2022) 86–95, https://doi.org/10.13448/j.cnki.jalre.2022.255.
[45] Department of natural resources of Jiangxi province, C. Overall Planning of Land and Space in Jiangxi province, China (2021-2035) [cited 2023 September 1, 2023]; Available from: http://bnr.jiangxi.gov.cn/art/2021/7/6/art_35804_3472745.html, 2021.
[46] Z. Wu, X. Chen, B. Liu, et al., Risk assessment of nitrogen and phosphorus loads in Hainan island based on InVEST model, Chin. J. Top. Crops 34 (9) (2013) 1791–1797, https://doi.org/10.3969/j.issn.1000-2561.2013.09.029.
[47] K.K. Kusi, A. Khattabi, N. Mhammdi, Evaluating the impacts of land use and climate changes on water ecosystem services in the Souss watershed, Morocco, Arabian J. Geosci. 16 (2) (2023) 126, https://doi.org/10.1007/s12517-023-11206-6.
[48] Y. Zou, X. Dong, Y. Liu, et al., Analysis of the changes in water conservation in Jiangxi province from 2000 to 2020, and the determinant factors, Journal of Resources and Ecology 14 (5) (2023) 940–950, https://doi.org/10.5814/j.issn.1674-764x.2023.05.005.
[49] S. Zhang, R. Chen, X. Cheng, Spatiotemporal changes of water-related ecosystem services and the responses to land use changes of the Longxi River Basin, Chongqing, J. Soil Water Conserv. 37 (4) (2023) 173–183, https://doi.org/10.13870/j.cnki.stbcxb.2023.04.023.
[50] Z. Li, Y. Zhang, Y. Ba, et al., Cold and Hot Spots Identification for Carbon Sequestration Capacity, Water Yield and Soil Conservation Services of Vegetation in Yunnan Province, China Environmental Science, 2023, pp. 1–14, https://doi.org/10.19674/j.cnki.issn1000-6923.20230908.002.
[51] K. Wang, Y. Feng, C. Qiu, et al., Spatial and temporal evolution and drivers of ecosystem services in Beijing, Tianjin and the Beijing-Tianjin Ring urban agglomeration, Acta Ecol. Sin. 42 (19) (2022) 7871–7883, https://doi.org/10.5846/stxb202111203270.
[52] L. Meng, J. Guo, C. Sun, et al., Suitability evaluation of urban construction land based on supply and demand in Yangzhou City, Resour. Sci. 40 (1) (2018) 11–21, https://doi.org/10.18402/resci.2018.01.02.
[53] J. Yang, X. Huang, The 30 m annual land cover dataset and its dynamics in China from 1990 to 2019, Earth Syst. Sci. Data 13 (8) (2021) 3907–3925, https://doi.org/10.5194/essd-13-3907-2021.
[54] F. Du, S. Chen, J. Pu, Spatiotemporal coupling analysis of urbanization and ecosystem services in southeastern Fujian, Environmental Science (2023) 1–17, https://doi.org/10.13227/j.hjkx.202308118.
[55] H. Zhao, G. Liu, Z. Yang, et al., Ecosystem Services Assessment and Multi-Scenario Prediction in Liaoning Province from 2000 to 2020, Environmental Science, 2023, pp. 1–22, https://doi.org/10.13227/j.hjkx.202307237.